Vibrational spectra of pilocarpine hydrochloride crystals

R.R.F. Bento
Instituto de Física, Universidade Federal do Mato Grosso, Cuiabá-MT, Brazil

P.T.C. Freire*
Departamento de Física, Universidade Federal do Ceará, Fortaleza-CE, Brazil

A.M.R. Teixeira and J.H. Silva
Dep. Ciências Físicas e Biológicas, Universidade Regional do Cariri, Crato-CE, Brazil

J.A. Lima Jr.
Universidade Estadual do Ceará, Limoeiro do Norte-CE, Brazil

M.C.F. de Oliveira and M. Andrade-Neto
Dep. Química Orgânica e Inorgânica, Universidade Federal do Ceará, Fortaleza-CE, Brazil

N.R. Romero
Departamento de Farmácia, Universidade Federal do Ceará, Fortaleza-CE, Brazil

F.M. Pontes
Faculdade de Ciências, Universidade Estadual de São Paulo, Bauru-SP, Brasil
(Received on 15 November, 2008)

Pilocarpine is a natural substance with potential application in the treatment of several diseases. In this work Fourier Transform (FT)-Raman spectrum and the Fourier Transform infra red (FT-IR) spectrum of pilocarpine hydrochloride $C_{11}H_{17}N_2O_2^+.Cl^-$ were investigated at 300 K. Vibrational wavenumber and wave vector have been predicted using density functional theory (B3LYP) calculations with the 6-31 G(d,p) basis set. A comparison with experiment allowed us to assign most of the normal modes of the crystal.

Keywords: Raman scattering, infrared spectroscopy, normal modes, pilocarpine hydrochloride

1. INTRODUCTION

In recent years, there has been a growing interest in the study of spectroscopic properties of plant cells in order to identify their chemical constituents through non-destructive analysis [1]. The main researches deal with primary metabolites, i.e., substances essential for their growth, surviving and reproduction (among them, amino acids, proteins, carbohydrates, lipids and fatty acids). On the contrary, the investigation of the vibrational property of isolated secondary metabolites from plants (used as defense against parasite and diseases as well as used to reinforce reproductive processes) is still poorly explored, although many of them have potential application as therapeutic drugs [2,3].

Secondary metability pilocarpine ($C_{11}H_{17}N_2O_2$), an alkaloid extracted from the leaves of the South American shrubs *Pilocarpus jaborandi*, *Pilocarpus microphyllus* and other *Pilocarpus* species [4], is an imidazole derivative that exhibits some pharmacological activities. These activities include diaphoretic effects, stimulation of parasympathetic system [5], miotic action [6], being also used in ophthalmology [6,7]. The action of pilocarpine on the parasymphatetic nervous system has been extensively investigated and it is known that the substance act mainly as a cholinergic drug [8]. Despite of several therapeutic effects, pilocarpine is used clinically only to treat glaucoma [8].

Pilocarpine molecule, which contains both imidazole and γ- lactone rings forms two semi-organic compounds in the solid state phase, trichlorogermanate hermihydrate [9] ($C_{11}H_{17}N_2O_2$, $GeCl_3$,1/2H_2O) and hydrochloride ($C_{11}H_{17}N_2O_2^+.Cl^-$). [10] For both compounds it was discovered that the crystal structures are monoclinic, space group $P2_1$, although the conformation of the pilocarpine molecule itself differs significantly from one structure to the other [9,10].

From the biological point of view, pilocarpine hydrochloride has been used in certain eye diseases, as for exemple, in the treatment of intraocular hemorrhages, opacities of the vitreous and aqueous fluids [8], while trichlorogermanate hermihydrate pilocarpine presents a weak activity of muscarinic stimulants [11].

In this work an infrared analysis and a Raman scattering study in the spectral range 40 cm^{-1} to 4000 cm^{-1} of pilocarpine hydrochloride crystal obtained from *Pilocarpus trachyllophys* [4] is reported. In order to assign the normal modes of vibrations of the material a Density Functional Theory (DFT) calculation was performed.

2. EXPERIMENTAL

FT-Raman spectrum was taken using a Bruker RFS100/S FTR system and a D418-T detector, with the sample excited by means of the 1064 nm line of a Nd:YAG laser. Infrared spectrum was obtained by using an Equinox/55 (Bruker) Fourier Transformed Infrared (FTIR) spectrometer. FT-Raman and

*Electronic address: tarso@fisica.ufc.br

FT-IR spectra were collected from samples confined in screw cap standard chromatographic glass vials, at a nominal resolution of 4 cm^{-1} accumulating 60 scans per spectra and using a laser power of 150 mW.

3. COMPUTATIONAL METHOD

Density functional theory (DFT) calculations were carried out using the Gaussian *98* programme package [12]. The B3LYP functional was used with the 6-31 G(d,p) basis set. The calculations were performed using an isolated molecule of pilocarpine cation: $C_{11}H_{17}N_2O_2^+$. The structure obtained from the X-ray analyses of pilocarpine hydrochloride at 77 K was used as starting structure [10]. This structure was optimized and the vibrational wavenumbers were then calculated. The output file contained the optimized structure, the vibrational frequencies in the harmonic approximation, and the atomic displacements for each mode. At the optimized structure of the molecule, no imaginary frequency was obtained, proving that a true minimum of the potential energy surface was found. The calculated vibrational wave numbers were adjusted to compare with experimental Raman and IR frequencies.

4. RESULTS AND DISCUSSION

The crystal of pilocarpine hydrochloride at room temperature belongs to the monoclinic structure with $P2_1(C_2^2)$ space group, with Z=2, and lattice parameters a = 11.057 [10.965] *Å*, b = 9.212 [9.177] *Å*, c =6.697 [6.507] *Å* and β = 110.05 [109.19]^o o (where the values in brackets hold for the 77 K determination) [10].

Figure 1 shows the molecular structure of the pilocarpine hydrochloride ($C_{11}H_{17}N_2O_2^+.Cl^-$). The numbering of the atoms in Fig. 1 follows that of Codding [10] in which the *N*-methylated nitrogens (N_1) are separated from the ether oxigen by four carbon atoms and from the carbonyl oxygen by five atoms. This labelling will be used in describing the parameters for optimized structure and the molecular wave vectors. The distribution of the two molecules of pilocarpine hydrochloride in the unit cell is showed in Fig. 2.

Tables 1, 2 and 3 show respectively, bond distances, bond angles and some selected torsion angles for pilocarpine cation, $C_{11}H_{17}N_2O_2^+$, for optimized structure of the molecule (Cal) and that obtained from X-ray analysis (Exp) [10]. The results show that optimized structure was observed to reproduce the experiments with good agreement.

FT-Raman spectrum and the FT-infrared (IR) spectrum of pilocarpine hydrocholride $C_{11}\ H_{17}\ N_2O_2^+.Cl^-$ are presented in Figs. 3(a) and 3(b), respectively.

The molecule of pilocarpine hydrochloride has C_1 site symmetry, and therefore, 93 molecular vibrations among all 99 are allowed in the Raman spectrum. The couplings of vibrations due to the presence of two molecules in the unit cell give rise to twice greater number of modes in the crystal. The number of normal modes expected for the crystal is then, 198, distributed into irreducible representations of C_2 factor group as 99 (A + B); from these modes 99 A + 99 B modes are Raman active. Assuming that the weakness of the intermolecular coupling causes negligible factor group splitting, the task is simplified to the assignment of the 93 molecular modes. Table 4 lists a detailed description of assignments for vibrational wavenumbers of pilocarpine hydrochloride. In the first column the calculated values for the wavenumbers are given. We also present the experimental wavenumber values for the crystal obtained by FT-Raman and FT-IR spectroscopies (the second and third columns, respectively); the fourth column in Table 4 gives the assignment of the bands. In order to better visualise the vibrations, we refer to the two rings in the assignments of Table 4, as follows: imidazole ring type or 1-methylimidazole as **R1** and γ- lactone ring type or γ-butyrolactone as **R2**. The nomenclature employed in the classification of normal modes is given below the Table 4.

The assignment for pilocarpine hydrochloride shows that most of the bands observed through FT-Raman and FT-IR spectroscopies correspond to a mixture of vibrational modes. The mixture of modes is common in molecules of C_1 site sym-

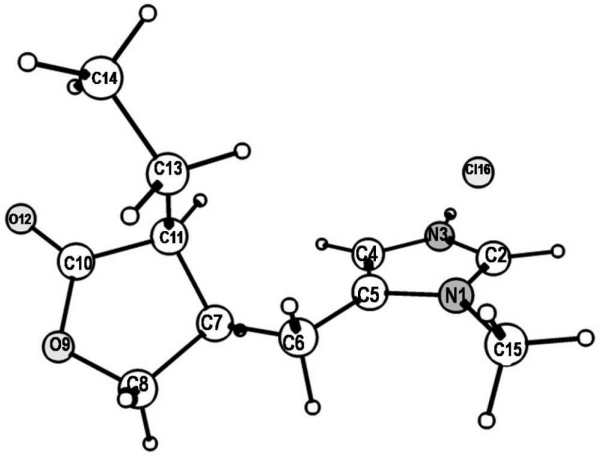

FIG. 1: The molecular structure of an isolated molecule of pilocarpine hydrochoride: $C_{11}\ H_{17}\ N_2O_2^+Cl^-$.

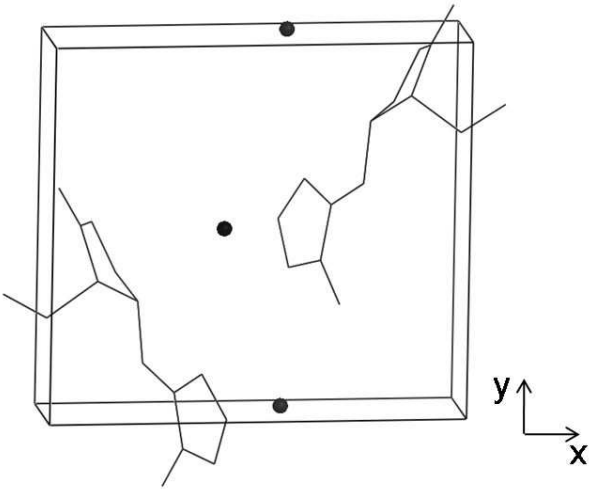

FIG. 2: Unit cell of pilocarpine hydrochloride; the Z plane is perpendicular to the figure.

TABLE 1: Bond distances ($\AA$) for Pilocarpine cation: $C_{11}\ H_{17}\ N_2O_2^+$.

	Exp.	Calc.
N(1)–C(2)	1.328	1.337
N(1)-C(5)	1.384	1.399
N(1)-C(15)	1.459	1.469
C(2)-N(3)	1.327	1.335
N(3)-C(4)	1.383	1.381
C(4)-C(5)	1.362	1.369
C(5)-C(6)	1.488	1.498
C(6)-C(7)	1.523	1.535
C(7)-C(8)	1.530	1.543
C(7)-C(11)	1.544	1.549
C(8)-O(9)	1.446	1.431
O(9)-C(10)	1.354	1.368
C(10)-C(11)	1.513	1.537
C(10)-O(12)	1.206	1.200
C(11)- C(13)	1.537	1.548
C(13) C(14)	1.526	1.533

TABLE 2: Bond angles ($^\circ$) for Pilocarpine cation: $C_{11}\ H_{17}\ N_2O_2^+$.

	Exp.	Calc.
C(2)-N(1)-C(5)	109.3	109.4
C(2)-N(1)-C(15)	124.7	124.9
C(5)-N(1)-C(15)	126.0	125.7
N(1)-C(2)-N(3)	108.5	107.9
C(2)-N(3)-C(4)	108.9	109.5
N(3)-C(4)-C(5)	107.0	107.2
N(1)-C(5)-C(4)	106.3	105.9
N(1)-C(5)-C(6)	121.8	122.5
C(4)-C(5)-C(6)	131.7	131.6
C(5)-C(6)-C(7)	113.4	114.2
C(6)-C(7)-C(8)	110.0	111.9
C(6)-C(7)-C(11)	118.3	118.7
C(8)-C(7)-C(11)	102.3	101.9
C(7)-C(8)-O(9)	105.0	105.3
C(8)-O(9)-C(10)	110.2	111.0
O(9)-C(10)-C(11)	110.9	109.7
O(9)-C(10)-O(12)	120.4	122.5
C(11)-C(10)-O(12)	128.6	127.9
C(7)-C(11)-C(10)	101.6	101.4
C(7)-C(11)-C(13)	114.6	116.2
C(10)-C(11)-C(13)	109.6	110.4
C(11)-C(13)-C(14)	114.7	113.5

metry. The superposition of modes precludes a direct identification of the bands. However, an effort was carried out through this work to make a detailed description of assignments of vibrational modes of the crystal. In order to illustrate the assignment, atomic displacements corresponding to selected normal modes from the isolated molecular structure of pilocarpine hydrochloride are shown in Fig. 4.

Now we discuss the main calculated and observed vibrations of pilocarpine hydrochloride. Two fundamental units of the pilocarpine molecule are the rings. Imidazole ring, which is a characteristic part of pilocarpine, is present in several substances of biological interest, as for example, L-histidine amino acid [13-15], and in other substances [16,17]. Their vibrations spread over a large spectral range of wavenumbers. Lactone, the other ring, is also found in several different substances of biological interest [18-20]; for some of them spectroscopic studies have revealed the wavenumber of the main vibrations [19]. Calculations show that at low wavenumber ($\omega < 150$ cm^{-1}) where it is expected to be observed bands associated to lattice vibrations, some internal modes are also present. For example, torsional vibrations of the two rings are observed together with lattice modes at very low wavenumber. This should be expected because the rings are very large structures; so, we assign the bands in this spectral region as a mixture of lattice modes and torsional vibrations of the rings R1 and R2. Fig. 4(a) shows atomic displacements associated to deformations $\{\gamma_{oop}$ (R1), δ_{oop} (R2) [τ (C10O9O12)], r(C13H$_2$), r(C14H$_3$)$\}$ corresponding to the strong Raman bands observed at 96 cm^{-1} (ω_{cal} = 97 cm^{-1}) .

Another class of vibrations is related to deformation of rings. In plane ring deformation vibration appears in a large spectral region (690 – 1900 cm^{-1}) and out of plane ring deformation vibration appears for $546 < \omega < 1140$ cm^{-1}. However, most of them are mixed with other kind of vibrations such as rocking and bending of CH, torsion of CH$_2$ and stretching of CC. Fig. 4(b) represents the mixtures of vibrational modes $\{\delta_{ip}$ (R2) [sc(C8C7C11); ν_s (C11C10O9)], r(C8H$_2$; C13H$_2$), r(C14H$_3$), δ(C7H)$\}$ giving rise to the strong Raman peak ob-

TABLE 3: Some selected torsion angles(°) for Pilocarpine cation: C_{11} H_{17} $N_2O_2^+$.

	Exp.	**Calc.**
C(2)-N(1)-C(5) –C(6)	176.7	179.1
C(3)-C(4)-C(5) –C(6)	-176.3	-178.9
N(1)-C(5)-C(6) –C(7)	179.8	177.2
C(4)-C(5)-C(6) –C(7)	-4.2	-4.1
C(5)-C(6)-C(7) –C(8)	168.4	171.6
C(5)-C(6)-C(7) –C(11)	-74.5	-70.1
C(6)-C(7)-C(8) –O(9)	157.0	159.2
C(6)-C(7)-C(11) –C(10)	-149.7	-153.3
C(6)-C(7)-C(11) –C(13)	-31.6	-33.5
C(7)-C(8)-O(9) –C(10)	-20.4	-20.2
O(9)-C(10)-C(11) –C(7)	18.2	19.8
O(12)-C(10)-C(11) –C(7)	-162.8	-161.2
C(7)-C(11)-C(13) –C(14)	171.4	179.4

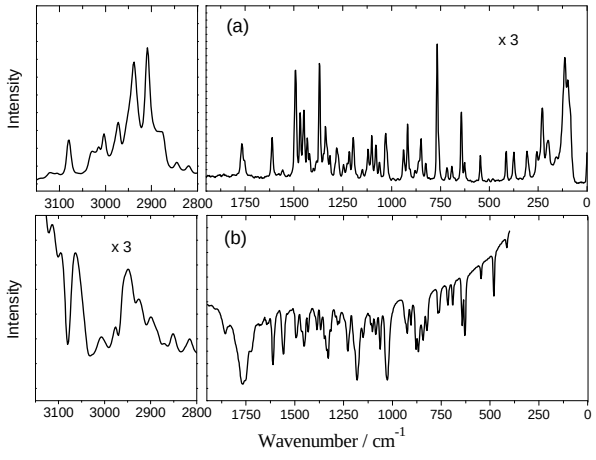

FIG. 3: (a) Pilocarpine hydrochloride FT-Raman spectrum. (b) Pilocarpine hydrochloride FT-IR spectrum.

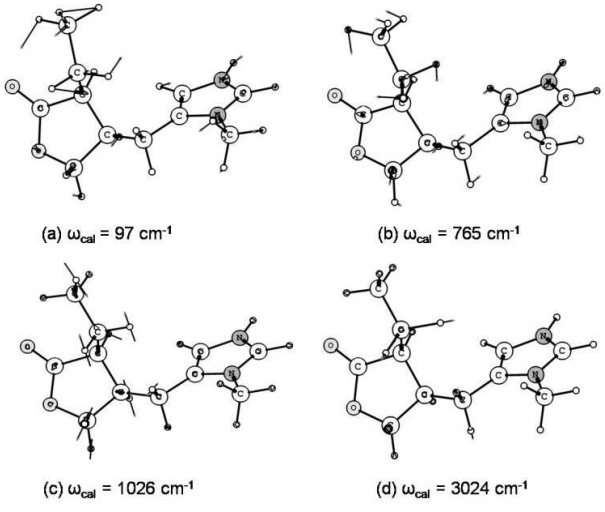

FIG. 4: Some selected representations of atomic vibrations corresponding to the strongest Raman bands of pilocarpine cation: C_{11} H_{17} $N_2O_2^+$.

served at 766 cm^{-1} ($\omega_{cal.}$ = 765 cm^{-1}).

The whole structure presents deformation vibrations δ(all structure) at $\sim$ 650 cm^{-1} as well as at $\sim$ 1080 cm^{-1} and at 1300 - 1340 cm^{-1}. A calculated δ (all structure) vibrational is also expected at 770 cm^{-1} but, possibly, is mixed with the 765 cm^{-1} complex vibration. Four strong IR bands are associated to ring deformation. Fig. 4(c) illustrates one of them observed at 1027 cm^{-1} (ω_{cal} = 1026 cm^{-1}), corresponding to $\{\delta_{oop}$ (R2) [ν_{as} (C11C13C14)], wag ($C13H_2$), r ($C6H_2$; $C8H_2$), r ($C14H_3$), δ (C7H; C11H)$\}$. Another band is observed at 1181 cm^{-1} (ω_{cal} = 1185 cm^{-1}), corresponding to $\{\delta_{ip}$ (R2) [sc (C8C7C11), ν (C10O9)], r ($C13H_2$), r ($C14H_3$), wag ($C6H_2$; $C8H_2$), δ (C7H; C11H)$\}$. The other two strong IR bands are associated with the deformations $\{\delta_{ip}$ (R1) [ν (N1C15; N3C2), ν (C4C5)], wag ($C15H_3$), δ (C2H; C4H), δ (N3H)$\}$ and $\{\delta_{ip}$ (R1) [ν (C4C5; C5C6), ν (C2N1)], wag ($C6H_2$), r ($C15H_3$), δ (C2H; C4H), δ (N3H)$\}$, corresponding to the peaks observed at 1752 cm^{-1} (ω_{cal} = 1598 cm^{-1}) and 1767 cm^{-1} (ω_{cal} = 1655 cm^{-1}), respectively.

It is also interesting to note that the rocking vibrations of the three CH_2 units ($C6H_2$, $C8H_2$ and $C13H_2$) are observed at similar wavenumbers. On the contrary, although CO_2 vibrations can be expected for pilocarpine molecule, rocking vibration of CO_2 (a well characteristic vibration in amino acid crystal at 500 – 540 cm^{-1}) is absent. This is because the only CO_2 possibility is C10O9O12, but O9 is held at lactone ring; as a consequence, it is impossible to have a rocking C10O9O12 vibration.

Because there are many C-C bonds in pilocarpine molecules the CC stretching vibrations are observed in a large range of wavenumbers. The lowest wavenumber value is for C11-C13 stretching, which was observed at 716 cm^{-1} while the highest wavenumber value corresponding to a ν(CC) is calculated at 1140 cm^{-1}.ν(NC) vibrations contributes with bands observed at 939 and 1754 cm^{-1}.

It is possible to note a marked localization of the scissoring vibrations (CH_2 and CH_3) in the range 1382 $cm^{-1} < \omega_{cal} <$ 1537 cm^{-1}. As an example, the Raman band observed at 1492 cm^{-1} (ω_{cal} = 1493 cm^{-1}) corresponds to the scissoring vibration sc($C15H_3$).

A large number of bands associated with overtones and combination tones may be found in the region about 2800 cm^{-1} due to the large number of bands in the region between 84 cm^{-1} and 1800 cm^{-1}. The bands 2819, 2834 and 2844

TABLE 4: Calculed vibrational wavenumbers unscaled, Raman band positions in units of cm^{-1} and assignments for vibrational modes of pilocarpine hydrochloride cation: $C_{11}\ H_{17}\ N_2O_2^+$.

ω_{calc}	$\omega_{FT-Raman}$	ω_{FT-IR}	*Assignment*
29			γ_{oop} (R1), r (C11C13C14)
43			γ_{oop} (R1), γ_{oop} (R2)
64	84m		γ_{oop} (R1), γ_{oop} (R2)
97	96s		γ_{oop} (R1), δ_{oop} (R2) [τ (C10O9O12)], r ($C13H_2$) , r ($C14H_3$)
123	114s		γ_{ip} (R1), δ_{oop} (R2) [τ (C10O9O12)], r ($C13H_2$) , r ($C14H_3$)
132			τ ($C15H_3$)
177	159w		γ_{oop} (R1), r (C11C13C14)
192	199w		γ_{oop} (R1), δ_{oop} (R2) [δ (C8O9)], r ($C8H_2$), r ($C14H_3$)
212			γ_{oop} (R1), γ_{oop} (R2), r (C11C13C14), δ (C15N1)
214			γ_{oop} (R1), δ_{oop} (R2) [δ(C10O12)], r ($C8H_2$), r ($C14H_3$; $C15H_3$)
228	229m		γ_{oop} (R1), δ_{oop} (N1C15), r ($C6H_2$), r ($C14H_3$)
247	256w		γ_{oop} (R1), γ_{ip} (R2), δ_{oop} (N1C15), r ($C6H_2$), r ($C14H_3$)
288			γ_{oop} (R1), δ_{oop} (N1C15), r ($C6H_2$; $C8H_2$; $C13H_2$); r ($C14H_3$)
298	306w		γ_{oop} (R1), γ_{oop} (R2), r ($C6H_2$; $C8H_2$; $C13H_2$); r ($C14H_3$)
366	374w		sc (C11C13C14), γ_{oop} (R2), r ($C6H_2$)
412	414w	415vw	γ_{ip} (R1), δ_{ip} (N1C15), δ_{oop} (R2)
479		480m	δ (all structure)
548	546w	546w	δ_{oop} (R2) [sc (C6C7C11); sc (O9C10O12)], r ($C6H_2$; $C8H_2$)
621			δ_{oop} (R1) [δ (C4N3C2)]
627	625vw	628m	δ (all structure)
641	643m	643m	δ (all structure)
654			δ_{oop} (R1) [δ(C4C5N1)], δ_{oop} (C2H; C4H), δ_{oop} (N3H), τ ($C6H_2$), r ($C8H_2$; $C13H_2$), r ($C15H_3$)
685			δ_{oop} (N3H)
690	691vw	690w	δ_{ip} (R2) [ν_s (C8O9C10)], r ($C6H_2$; $C8H_2$; $C13H_2$), r ($C14H_3$)
710	716vw	716w	δ_{oop} (R2) [δ_{oop} (C10O12)], ν (C11C13), δ (C11H) , r ($C13H_2$), r ($C14H_3$)
765	766s	762w	δ_{ip} (R2) [sc (C8C7C11); ν_s (C11C10O9)], r ($C8H_2$; $C13H_2$), r ($C14H_3$), δ (C7H)
770			δ (all structure)
787	824vw	822m	δ_{oop} (R1) [δ_{oop} (C2H; C4H)], r ($C6H_2$)
834	850w	843m	δ_{oop} (C2H; C4H), δ_{oop} (N3H)
852	861vw	866m	δ_{oop} (R2) [n (C11C13); ν_s (C8C7C11)], τ ($C13H_2$), r ($C14H_3$), δ (C7H; C11H)
880		880m	δ_{ip} (R2) [δ (C10O12); ν_s (C11C10O9)], τ ($C8H_2$; $C13H_2$), r ($C14H_3$), δ_{oop} (C4H)
917	918m	905w	δ_{oop} (R2) [ν_s (C11C13C14), ν (C7C8)], δ_{oop} (C4H), δ (C7H)
939	939w	927w	δ_{ip} (R1) [ν (C5N1), sc (C2N3C4)], r ($C15H_3$)
950			δ_{oop} (R2) [ν_s (C11C13C14), ν (C7C8)], δ (C7H; C11H), r ($C6H_2$; $C8H_2$), r ($C14H_3$)
1026	1031m	1027s	δ_{oop} (R2) [ν_{as} (C11C13C14)], wag ($C13H_2$), r ($C6H_2$; $C8H_2$), r ($C14H_3$), δ (C7H; C11H)
1039			δ_{ip} (R2) [ν(C7C8)], ν_{as}C11C13C14), wag ($C6H_2$), r ($C8H_2$), δ (C11H)
1068	1063w	1063m	δ_{oop} (R2) [ν(C7C8; C10O9)], r ($C6H_2$; $C13H_2$); r ($C14H_3$) , δ (C2H; C4H; C11H), δ (N3H)
1078			δ (all structure)
1083	1081w	1085w	δ (all structure)
1106	1102w	1103w	δ_{oop} (R2) [r (C7C11C13); ν (C8O9; C10O9)], ν (C13C14), r ($C14H_3$), τ ($C13H_2$), δ (C7H; C11H)
1124	1121w		δ_{ip} (R1) [ν (C4N3)], r ($C15H_3$), ν (C7C11), δ (C2H; C4H)
1126			δ_{ip} (R1) [ν (C5N1; C4N3)], r ($C14H_3$; $C15H_3$), r ($C8H_2$), ν (C7C11) d (N3H)
1140			δ_{oop} (R2) [n (C11C13)], r ($C14H_3$; $C15H_3$), r ($C8H_2$), δ (C2H; C4H), δ (N3H)
1152	1151vw	1150w	r ($C15H_3$), δ (C2H; C4H), δ (N3H)
1153			δ (all structure)
1185		1181s	δ_{ip} (R2) [sc (C8C7C11), ν (C10O9)], r ($C13H_2$), r ($C14H_3$), wag ($C6H_2$; $C8H_2$), δ (C7H; C11H)
1207	1196m		δ_{ip} (R1) [sc (C5C4N3)], wag ($C6H_2$), r ($C8H_2$), δ (C2H; C4H; C7H; C11H), δ (N3H)
1235	1218w	1228m	r ($C14H_3$), τ ($C6H_2$; $C8H_2$), δ (C2H; C7H; C11H)
1253	1245vw		r ($C14H_3$), τ ($C6H_2$; $C8H_2$), δ (C4H; C7H; C11H), δ (N3H)
1267		1272vw	δ_{ip} (R1) [ν (C4N3)], r ($C14H_3$), τ ($C8H_2$; $C13H_2$), δ (C2H; C4H; C7H; C11H), δ (N3H)

cm^{-1} were assigned as combination tone. The intensity of bands at 2844 cm^{-1} suggests that is a combination involving

Table 4 (Continued)

ω_{calc}	$\omega_{FT-Raman}$	ω_{FT-IR}	*Assignment*
1280	1279w	1281vw	δ_{ip} (R1) [ν (C4N3)], r ($C14H_3$; $C15H_3$), τ ($C6H_2$; $C13H_2$), δ (C2H; C4H; C7H; C11H), δ (N3H)
1306		1292vw	δ (all structure)
1310	1315w		δ (all structure)
1339	1337m	1331m	δ (all structure)
1349			τ ($C6H_2$; $C8H_2$; $C13H_2$), δ (C11H), r ($C14H_3$)
1371	1369s	1367w	wag ($C14H_3$), wag ($C13H_2$), τ ($C6H_2$; $C8H_2$), ν_{as}(C11C13C14), r (C5C6C7), δ (C2H; C7H; C11H), δ (N3H)
1382	1387vw	1387w	sc ($C14H_3$), τ ($C6H_2$; $C8H_2$), wag ($C13H_2$), ν_{as}(C11C13C14), δ (C7H; C11H)
1392			δ_{ip} (R1) [sc (C4C5N3); ν (N1C2; N1C5)], sc ($C15H_3$), wag ($C6H_2$; $C8H_2$; $C13H_2$), ν_{as}(C5C6C7), δ (C7H)
1408			wag ($C14H_3$), wag ($C6H_2$; $C8H_2$; $C13H_2$), sc ($C15H_3$) δ (C7H)
1424	1422vw		wag ($C14H_3$), wag ($C6H_2$; $C8H_2$; $C13H_2$), δ (C7H; C11H)
1438	1433w	1432w	wag ($C14H_3$)
1468	1449m	1452m	wag ($C15H_3$), sc ($C6H_2$), δ (C2H), δ (N3H)
1480	1468m		sc ($C14H_3$; $C15H_3$), sc ($C6H_2$; $C13H_2$)
1493	1492s	1492w	sc ($C15H_3$)
1506			sc ($C14H_3$; $C15H_3$), sc ($C6H_2$; $C13H_2$)
1511			sc ($C14H_3$; $C15H_3$), sc ($C13H_2$), δ (N3H)
1512			sc ($C14H_3$; $C15H_3$), sc ($C13H_2$), δ (N3H), δ_{ip} (R1) [ν (C2N3; C4N3)]
1518			sc ($C14H_3$; $C15H_3$), sc ($C6H_2$; $C13H_2$), δ (N3H)
1523	1559vw	1558m	sc ($C14H_3$), sc ($C13H_2$)
1537	1611w	1613m	sc ($C8H_2$)
1598	1754vw	1752s	δ_{ip} (R1) [ν (N1C15; N3C2), ν (C4C5)], wag ($C15H_3$), d (C2H; C4H), δ (N3H)
1655	1767w	1767s	δ_{ip} (R1) [ν (C4C5; C5C6), ν (C2N1)], wag ($C6H_2$), r ($C15H_3$), δ (C2H; C4H), δ (N3H)
1892		1863w	δ_{ip} (R2) [ν_s (C10=O12)]
	2819w		combination
		2834vw	combination
	2844w		combination
3024	2908vs	2911vw	ν_s ($C6H_2$; $C13H_2$), ν (C7H)
3027	2938vs	2935vw	ν_s ($C6H_2$; $C8H_2$; $C13H_2$), ν (C7H)
3036	2972s	2970w	ν_s ($C6H_2$; $C8H_2$; $C13H_2$), ν (C7H; C11H)
3045	3004s	3007w	ν_{as} ($C6H_2$), ν_s ($C8H_2$) , ν (C7H; C11H)
3055	3025m	3030w	ν_s ($C14H_3$), ν_{as} ($C13H_2$), ν (C11H)
3061			ν_s ($C14H_3$), ν_{as} ($C6H_2$; $C13H_2$), ν_s ($C8H_2$) , ν (C11H)
3077	3079s		ν_s ($C15H_3$), ν_{as} ($C6H_2$; $C13H_2$), ν (C7H; C11H)
3084			ν_s ($C15H_3$), ν_{as} ($C13H_2$), ν (C7H; C11H)
3085			ν_s ($C15H_3$), ν_{as} ($C6H_2$; $C13H_2$), ν (C7H; C11H)
3124	3116vw		ν_{as} ($C14H_3$), ν_{as} ($C6H_2$; $C13H_2$), ν (C7H; C11H)
3125			ν_{as} ($C14H_3$), ν_{as} ($C8H_2$; $C13H_2$), ν (C7H; C11H)
3157			ν_{as} ($C14H_3$), ν_{as} ($C13H_2$)
3170			ν_{as} ($C15H_3$)
3188			ν_{as} ($C15H_3$)

τ = twisting; γ = torsion; sc= scissoring; wag = wagging; δ = deformation; δ_{ip} = deformation in plane; δ_{oop} = deformation out of plane; r = rock; ν = stretching; ν_{as} = asymmetric stretching; ν_s = symmetric stretching. vs=very strong ; s = strong; m = medium; w = weak; vw =very weak.

at least one strong Raman band. Thus, the modes at 96, 114, 766, 1369, and 1492 cm^{-1} can be involved.

The spectral region between 2800 and 3150 cm^{-1} of the Raman spectrum of pilocarpine hydrochloride crystal consists of a series of very intense Raman bands, and a series of less intense IR bands. However, all bands are well resolved, allowing for their identification as listed in Table 4. For organic crystals the region about 3000 cm^{-1}, in general, contains the bands originated from C-H, CH_2, CH_3, and N-H vibrations [21, 22]. For some materials this region condenses very important informations, being a tool to understand conformation of the molecules in the unit cell or even interactions such as hydrogen bonds. For example, a study on L-methionine crystal have shown that the behaviour of Raman bands under pressure in this spectral region can be understood as consequence of structural changes instead of simple conformational changes of molecules in the unit cell [23]. So, the understand of the origin of these bands can be fundamental to understand the behaviour of pilocarpine hydrochloride under different conditions, in particular, related to the conditions found in drug artefacts. The scheme of Fig. 4(d) shows, as an example, the mixtures of stretching modes $\{\nu_s(C6H_2;\ C13H_2),\ \nu\ (C7H)\}$ corresponding to a very strong Raman band observed at 2908 cm^{-1} (ω_{cal} = 3024 cm^{-1}).

5. CONCLUSIONS

The phonon spectrum of the pilocarpine hydrochloride, a potential pharmaceutical substance to be used in several dis-

ease treatments, was measured at room temperature through FT-Raman and FT-IR techniques. Density functional theory calculations were carried out by using the Gaussian *98* package and the B3LYP functional with the 6-31 G(d,p) basis set. The calculations were observed to reproduce the experiments with good agreement. This agreement allowed us the assignment of the observed wavenumbers to atomic motions in the molecules. In particular, it was observed that most bands are associated to mixing of vibrational modes, even in the low wavenumber region where, generally, the lattice modes are found. The absence of stretching vibrations of water molecule which can be observed at ~ 3400 cm^{-1} in this region indicates that the crystal is free of water molecules.

Acknowledgments

We thank CENAPAD-SP for the use of the GAUSSIAN 98 software package and for computational facilities through the project reference "proj373"**.** Financial support from CNPq, CAPES and FUNCAP is also acknowledged. One of us (AMRT) thanks Universidade Regional do Cariri for allowing him to spend one year at UFC to develop his pos-doc research.

[1] E. Urlaub, J. Popp, W. Kiefer, G. Bringmann, D. Koppler, H. Schneider, U. Zimmermann, and B. Schrader. Biospectrosc. **4**, 113 (1998).
[2] R.J.H. Clark, R.E. Hester (eds). *Spectroscopy of Biological Systems. Advances in Spectroscopy*, vol. 13. Wiley: Chichester, 1986.
[3] W. Sneader. *Drug Prototypes and their Exploitation*. Wiley: Chichester, 1996.
[4] M. Andrade-Neto, E.R. Silveira, P.H. Mendes. Phytochem. **42**, 885 (1996).
[5] B. Levy, R.P. Ahliquist. J. Pharmacol. Erp. Ther. **137**, 219 (1962).
[6] P.G. Watson. Br. J. Ophthalmol. **56**, 145 (1972).
[7] B.N. Schwartz. Engl. J. Med. **290**, 182 (1978).
[8] L.S. Goodman, A. Gilman. *The Pharmacological Basis of Therapeutics*, 6th ed.; MacMillan: New York, 1980; p 97.
[9] S. Fregerslev, S.E. Rasmussen. Acta Chem. Scand. **22,** 2541 (1968).
[10] P.W. Codding, M.N.G. James. Acta Crystallogr. **B40**, 42 (1984).
[11] J.M. Schulman, M.L. Sabio, R.L. Disch. J. Med. Chem. **26**, 817 (1983)**.**
[12] M.J. Frisch, G.W. Trucks, H.B. Schlegel, G.E. Scuseria, M.A. Robb, J.R. Cheeseman, V.G. Zakrzewski, J.A. Montgomery, R.E. Stratmann Jr, J.C. Burant, S. Dapprich, J.M. Millam, A.D. Daniels, K.N. Kudin, M.C. Strain, O. Farkas, J. Tomasi, V. Barone, M. Cossi, R. Cammi, B. Mennucci, C. Pomelli, C. Adamo, S. Clifford, J. Ochterski, G.A. Petersson, P.Y. Ayala, Q. Cui, K. Morokuma, P. Salvador, J.J. Dannenberg, D.K. Malick, A.D. Rabuck, K. Raghavachari, J.B. Foresman, J. Cioslowski, J.V. Ortiz, A.G. Baboul, B.B. Stefanov, G. Liu, A. Liashenko, P. Piskorz, I. Komaromi, R. Gomperts, R.L. Martin, D.J. Fox, T. Keith, M.A. Al-Laham, C.Y. Peng, A. Nanayakkara, M. Challacombe, P.M.W. Gill, B. Johnson, W. Chen, M.W. Wong, J.L. Andres, C. Gonzalez, M. Head-Gordon, E.S. Replogle, J.A. Pople. Gaussian 98 (Revision A.11.2). Gaussian: Pittsburgh, PA, 2001.
[13] M. Tasumi , I. Harada, T. Takamatsu, S. Takahashi. J. Raman Spectrosc. **12**, 149 (1982).
[14] T. Miura, T. Satoh, A. Hori-i, H. Takeuchi. J. Raman Spectrosc. **29**, 41 (1998).
[15] J.L.B. Faria, F.M. Almeida, O. Pilla, F. Rossi, J.M. Sasaki, F.E.A. Melo, J.M. Filho, P.T.C. Freire. J. Raman Spectrosc. **35**, 242 (2004).
[16] A. Torreggiani, A. Degli Esposti, M. Tamba, G. Marconi, G. Fini , J. Raman Spectrosc. **37**, 291 (2006).
[17] B.H. Loo, Y. Tse, K. Parsons, C. Adelman, A. El-Hage, Y.G. Lee, J. Raman Spectrosc. **37**, 299 (2006).
[18] W. Zhang, K. Krohn, J. Ding, Z.H. Miao, X.H. Zhou, S.H. Chen, G. Pescitelli, P. Salvadori, T. Kurtan, Y.W. Guo. J. Nat. Prod. **71**, 961 (2008).
[19] J. Binoy, J.P. Abraham, Joe I. Hybert, V. George, V.S. Jayakumar, J. Aubard, Nielsen O. Faurskov. J. Raman Spectrosc. **36**, 63 (2005).
[20] S. Basu, Y. Gerchman, C.H. Collins, F.H. Arnold, R. Weiss, Nature **434**, 1130 (2005).
[21] B.L. Silva, P.T.C. Freire, F.E.A. Melo, I. Guedes, M.A.A. Silva, J.M. Filho, A.J.D. Moreno. Braz. J. Phys. **28**, 19 (1998).
[22] P.F. Façanha Filho, P.T.C. Freire, K.C.V. Lima, J.M. Filho, F.E.A. Melo, P.S. Pizani. Braz. J. Phys. **38**, 131 (2008).
[23] J.A. Lima Jr., P.T.C. Freire, F.E.A. Melo, V. Lemos, J. Mendes-Filho, P.S. Pizani. J. Raman Spectrosc. **39**, 1356 (2008).